

Determination of spatial quantum states by using Point Diffraction Interferometry.

Quimey Pears Stefano,^{1,2,*} Lorena Rebón,³ and Claudio Iemmi^{1,2}

¹*Universidad de Buenos Aires, Facultad de Ciencias Exactas y Naturales,
Departamento de Física, Buenos Aires, Argentina.*

²*Consejo Nacional de Investigaciones Científicas y Técnicas, Buenos Aires, Argentina.*

³*Departamento de Física, IFLP-CONICET, Universidad Nacional de La Plata, C.C. 67, 1900 La Plata, Argentina.*

(Dated: February 9, 2022)

We present a method to reconstruct pure spatial qudits of arbitrary dimension d , which is based on a point diffraction interferometer. In the proposed scheme, the quantum states are codified in the discretized transverse position of a photon field, once they are sent through an aperture with d slits, and a known background is added to provide a phase reference. To characterize these photonic quantum states, the complete phase wavefront is reconstructed through a phase-shifting technique. Combined with a multipixel detector, the acquisition can be parallelized, and only four interferograms are required to reconstruct any pure qudit, independently of the dimension d . We tested the method experimentally, for reconstructing states of dimension $d = 6$ randomly chosen. A mean fidelity values of 0.95 is obtained. Additionally, we develop an experimental scheme that allows to estimate phase aberrations affecting the wavefront upon propagation, and thus improve the quantum state estimation. In that regard, we present a proof-of-principle demonstration that shows the possibility to correct the influence of turbulence in a free-space communication, recovering mean fidelity values comparable to the propagation free of turbulence.

I. INTRODUCTION

Quantum information processing is a research area in constant growth, mainly stimulated by promising applications such as: quantum metrology [1], quantum computation [2], quantum networks [3], quantum cryptography [4] and fundamental tests of quantum mechanics [5, 6]. Therefore, determining the unknown state of a quantum system is an essential task for the development of these emerging applications, as well as to compare and validate their performance. Usually, the schemes for the complete characterization of a quantum system, collectively named as quantum state tomography (QST) methods, rely on the result of multiple measurements on identical copies of the unknown state to estimate its density matrix ρ . For a quantum system of dimension d (qudit) there are $d^2 - 1$ independent elements to be determined in order to reconstruct ρ , posing a scale problem for typical QST methods [7–9] since they require a number of measurements that scales as $\sim d^2$.

Despite that, many applications can be improved using high-dimensional quantum systems [10–16] which pushes increasingly to develop new QST schemes that require fewer measurements. For example, if some information about the state is known *a priori*, a reduction in the number of measurements is feasible. In fact, several works have demonstrated that pure quantum states can be accurately reconstructed from a number of measurements that scales as $\sim d$ [17–19]. Although, in general, an arbitrary quantum system will be in a mixed state, the reconstruction of pure states is especially important since most current applications of quantum information are based on pure states.

Among the several physical implementations of a quantum state, photonic systems are ideally to be used for quantum communications applications [20]. Particularly, the discretized transverse momentum of single photons was used to define photonic quantum states, usually called *slit states* [21–24]. This is a very versatile option for the encoding of quantum states that allows to achieve high dimensional Hilbert spaces, easily in relation to other codifications. In this context, we have previously proposed and demonstrated [23] a QST method to reconstruct pure slit states of dimension $d > 2$ based on the phase shifting interferometry (PSI) technique. As remarkable feature, that scheme requires a minimum number of measurements, $4d$, and depending on the used optical architecture, it can be parallelized with the acquisition of only four interferograms, independently of the system dimension d .

Following the strategy of using interferometric techniques for pure QST from a reduced number of measurements, we propose here a PSI scheme based on a point diffraction interferometer (PDI) as a new tool for high-quality estimation of photonic quantum states. The PDI technique, introduced by Linnik in reference [25], uses a common-path configuration where the reference beam is generated from the same wavefront under characterization. Its common-path feature results on an interferometer extremely stable against vibrations and air turbulence. It has been applied for testing optical components in a wide range of wavelengths, from infrared [26] to extreme ultraviolet [27]. When combined with PSI schemes, for example by using liquid crystal technology [28–30] to control the phase steps, the potential applications of this interferometer are enhanced. For instance, in reference [29] Iemmi *et al* used a commercial liquid crystal display (LCD) to implement a PDI scheme that allows to correct *in situ* the aberrations in a Vander Lugt

* quimeyps@df.uba.ar

correlator, while in reference [30] the technique was used to obtain a digital holographic movie.

The architecture of the present device is very stable, requires relatively few optical elements, and it is easy to align. Moreover, since the detection is performed in the conjugated plane of the input wavefront, where the slit states are codified, it is possible to parallelize the measurements and carry out the tomographic process from only 4 measurements, regardless of the dimension of the quantum state. To implement this process, it is necessary to modify the encoding of the slit states, so that, the input signal includes a coherent background that acts as a reference for the interferograms. Thus, the technique allows evaluating all points of the wavefront and not only those belonging to the slits. This feature makes the method especially suitable for quantum communications in free space since it allows correcting the effect of turbulence-induced aberrations.

The article is organized as follows: in section II we review the fundamentals of PDI (II A) and propose an alternative encoding for the slit states that includes a reference beam (II B). In section III we describe the experimental common-path interferometer used to perform the quantum state reconstruction. In section IV, dedicated to the experimental results, we show the fidelity of reconstruction for a great number of quantum states. In particular, we devote subsection IV B to show the feasibility of this method to correct the effects of turbulence in free-space communication. Finally, in section V we give the conclusions.

II. DESCRIPTION OF THE METHOD

In this section we will describe the two main points on which the tomographic method is based. On one hand, we will briefly review the features of a PDI adapted for the implementation of PSI techniques, since it is an accurate and effective method for phase measurement. On the other hand, we will analyze how the encoding of the slit states should be modified, with respect to the standard one, in order to be correctly evaluated with the proposed device.

A. Point diffraction interferometer (PDI)

Let us describe the interferometric process following the sketch shown in figure 1. The input wavefront $U(x, y)$ is focused by the lens \mathbf{L}_1 at the Fourier transform plane Π_f . When no diffracting object or aberration is present, the resulting light distribution is a bright central spot, corresponding to the Fourier transform of the entrance pupil of the system. At Π_f , a phase filter $H(u, v)$, smaller than the focused spot, is placed (see inset in figure 1). This filter is used as a perturbation to generate a spherical wave by diffraction effect. When an object or aberration is present in the input signal, the bright spot is

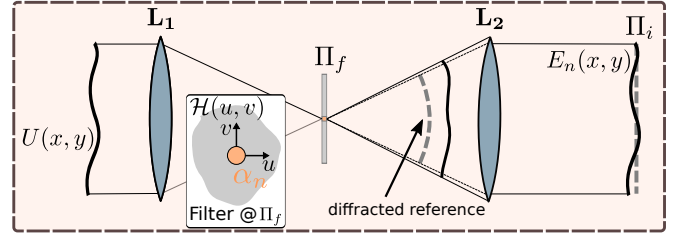


FIG. 1: Schematics of the working principle of a PDI. Lens \mathbf{L}_1 focus the input wavefront to be characterized $U(x, y)$ (wavy line) at the Fourier plane, Π_f . The phase filter at Π_f introduces a phase α_n in a small area in the center of the Fourier transform (see inset) given place to a reference wavefront (dashed line). Lens \mathbf{L}_2 images $U(x, y)$ onto the final plane Π_i , where the interference pattern $|E_n(x, y)|^2$ is registered.

deformed. Most of the light is diffracted towards higher spatial frequencies, and only the small central part of the spot go through the phase filter. In this way, after Π_f two waves will be present: an object wave (wavy line in the figure 1) and a reference wave (dashed line), which are going to interfere. Lens \mathbf{L}_2 images the object plane Π_i in such a way that the amplitude and phase distribution at the object plane can be evaluated.

The input wavefront $U(x, y)$ can be fully reconstructed by implementing a PSI scheme [31]. This technique consists in introducing successive controlled phase shifts α_n in the reference beam that interfere with the object beam, while the corresponding interferogram intensity is registered.

The transfer function that implements the phase shifts α_n can be described as

$$H(u, v) = 1 + \delta(u, v) [\exp(i\alpha_n) - 1], \quad (1)$$

where $\delta(\cdot)$ is the two dimensional Dirac function, (u, v) indicate the transverse coordinates at Π_f , and $\alpha_n = 2\pi n/N$ is the constant phase added to the reference in each of the N steps of a PSI scheme.

The amplitude at the image plane Π_i is

$$E_n(x, y) = U(x, y) \otimes h(x, y) = U(x, y) + K [e^{i\alpha_n} - 1], \quad (2)$$

where the symbol \otimes represents the convolution, $h(x, y)$ is the filter impulse response, and K is the complex constant corresponding to the mean value of $U(x, y)$. As the final aim of this method is to obtain the amplitude and the phase of $U(x, y)$, it is useful to rewrite $U(x, y) = u(x, y) \exp(i\phi(x, y))$, where $u(x, y)$ is the absolute value of $U(x, y)$ and $\phi(x, y)$ represents the phase. To fully reconstruct the input wavefront, $N > 3$ interferograms $E_n(x, y)$ ($n = 0, \dots, N$), have to be recorded with a multipixel detector, and the measurements intensities

are then combined in the expressions

$$C(x, y) = \sum_{n=0}^{N-1} |E_n(x, y)|^2 \cos\left(\frac{2\pi n}{N}\right) \quad (3)$$

$$S(x, y) = \sum_{n=0}^{N-1} |E_n(x, y)|^2 \sin\left(\frac{2\pi n}{N}\right). \quad (4)$$

Both expression can be simplified according to the orthogonality properties of the trigonometric functions:

$$C(x, y) = -N |K|^2 + N |K| u(x, y) \cos(\phi(x, y) + \mu) \quad (5)$$

$$S(x, y) = N |K| u(x, y) \sin(\phi(x, y) + \mu). \quad (6)$$

Thus, the unknown phase of the wavefront $\phi(x, y)$ can be reconstructed as

$$\phi(x, y) = \arctan2(S, C - C_0) - \mu, \quad (7)$$

where $\arctan2(x_1, x_0)$ is defined as the angle between the 2-dimensional vector (x_0, x_1) and the x_0 axis, μ is the global phase of K and $C_0 = -N |K|^2$. The value of C_0 can be readily obtained from the value of $C(x, y)$ at the points in which the input wavefront $U(x, y)$ is zero. Finally, the real amplitude of $u(x, y)$ is E_0 .

B. Encoding of the spatial photonic qudit

As we have explained in the previous subsection, the PDI method requires a nonzero DC component in the input light distribution that gives place to the reference wave, and for this purpose, we have to provide a background to the codified states.

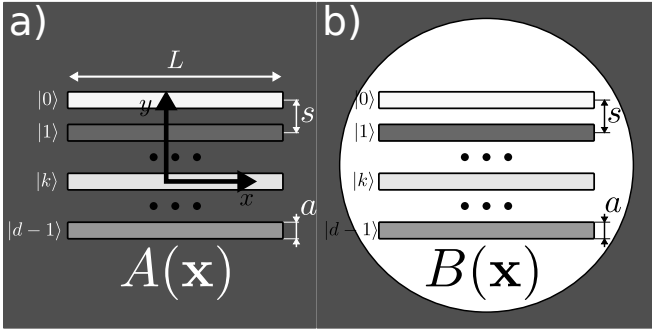


FIG. 2: Complex amplitude mask for an example slit state of arbitrary dimension d . The gray scale is only schematic, and the lighter zones represent greater transmissivity. (a) Standard definition of a slit state (equation (9)). (b) Proposed modification to the definition of the state in (a). The background acts as a reference for the PDI.

The formalism of slit states is described in detail in references [32–34]. Here we present a brief review of the

standard codification. Let $A(\mathbf{x})$ be the complex transmission function of an aperture. When a paraxial and monochromatic single-photon field, described by the normalized transverse probability amplitude $\psi(\mathbf{x})$, impinges on this aperture, the resulting quantum state is

$$|\Psi\rangle = \int d\mathbf{x} \psi(\mathbf{x}) A(\mathbf{x}) |1\mathbf{x}\rangle, \quad (8)$$

where $\mathbf{x} = (x, y)$ is the transverse position coordinate and $|1\mathbf{x}\rangle$ is the single-photon state in the position basis. We are interested in representing a quantum state of finite dimension d , and therefore, we must discretize the transverse position. Let us consider that $A(\mathbf{x})$ is an array of d rectangular slits of width a , where the separation between adjacent slits is s , and the length is $L (\gg a, s)$, that is:

$$A(\mathbf{x}) = \text{Rect}(x/L) \sum_{k=0}^{d-1} c_k \text{Rect}\left(\frac{y - ks}{a}\right), \quad (9)$$

where the $\{c_k\}_{k=0}^{d-1}$ are the complex transmission amplitudes of each rectangular region and $\text{Rect}(\eta)$ is the rect-angle function, that takes the value 1 if $|\eta| < 1/2$ and the value 0 otherwise. Figure 2a shows, schematically, the aperture given by equation (9). For simplicity we will assume that $\psi(\mathbf{x})$ is approximately constant across the region of the slits, and hence, the quantum state described by equation (8) is the qudit state

$$|\Psi\rangle = \sum_{k=0}^{d-1} c_k |k\rangle, \quad (10)$$

where $\{|k\rangle\}_{k=0}^{d-1}$ is the logical basis.

In order to have a light distribution similar to those usually present in an in-line holography process (small diffracting objects immersed in a strong background), we propose a modification on the representation of the slit states that includes a constant light background. These states can be thought of as generated by an aperture function $B(\mathbf{x})$ that is the same as $A(\mathbf{x})$ in the zones corresponding to every slit, but surrounded by a circular region of constant amplitude that introduces the required background. The modified aperture, schematically shown in figure 2b, is expressed as

$$B(\mathbf{x}) = A(\mathbf{x}) + \quad (11)$$

$$\text{Circle}(|\mathbf{x}|^2/R) \left[1 - \text{Rect}(x/L) \sum_{k=0}^{d-1} \text{Rect}\left(\frac{y - ks}{a}\right) \right],$$

where $\text{Circle}(\eta) = 1$ for $|\eta| < 1$ and 0 otherwise, and R is the radius of the background pupil.

It is worth remarking that, given a quantum state defined by $B(\mathbf{x})$, one can always obtain the usual slit state $|\Psi\rangle$ by postselection with an amplitude mask with unitary transmission in the slits rectangles, and zero elsewhere. Additionally, the proposed representation allows

to evaluate the amplitude and phase distribution over all the circular pupil. Later, in subsection IV B, we will show how to estimate the introduced phase aberrations on the photonic quantum state of interest due to its free propagation in a turbulent medium, and how to use this information for a corrected estimation of such a state.

III. EXPERIMENTAL IMPLEMENTATION

The experimental setup, depicted in figure 3, is basically a convergent optical processor in which two phase-only Spatial Light Modulators (SLMs) are used: one to prepare the input qudit state, and the other to dynamically introduce the phase retardation needed to implement the PSI process. Both SLMs are conformed by a Sony liquid crystal television panel model LCX012BL which, in combination with polarizers and wave plates, that provide the adequate state of light polarization, allows a 2π phase modulation of the incident wavefront [35]. This model of liquid crystal has a VGA resolution of 640×480 and a pixel size of $43 \mu\text{m}$. The light source is a laser diode @405nm, that is expanded by the microscope objective **O** and spatially filtered. Neutral density filters, not shown in the figure, attenuate the source to the single-photon level. The lens **L**₁ images the pinhole onto the Fourier plane Π_f . The aperture $B(\mathbf{x})$ that defines the spatial qudit is displayed, dynamically, in the phase-only **SLM**₁, which is placed in the object plane Π_o . The aperture was programmed so that each slit had a width a of 4 pixels and a separation s of 6 pixels. To generate the mask described in equation (11) by means of a pure phase modulator we use the method proposed in reference [33]. Briefly, the mask is encoded as a blazed phase diffraction grating, where the local phase depth controls the efficiency of the first diffraction order, and thus the local amplitude of the mask. The phase of the complex coefficients c_k are controlled by displacing the grating. If p is the period in pixels, the relative phase introduced by a displacement of k pixels is $2\pi \frac{k}{p}$. In our case, the grating period is $p = 12$, resulting in a sufficiently small discretization error [36]. The diffracted first order is selected by means of the spatial filter **SF**₁ (a slit of width $\approx 200 \mu\text{m}$), which is placed at the Π_f plane. The lens **L**₂ images the filtered Π_o complex distribution onto the plane Π_i .

SLM₂ is placed in plane Π_f , right after the spatial filter **SF**₁. We use this modulator to represent the phase filter $\mathcal{H}(u, v)$ given by equation (1)), i.e., the phase shifts α_n needed to implement the PSI technique are introduced in the central pixel. The inset in figure 3 shows a detail of such filters: the pixel that introduces the phase α_n to the reference (the dashed one within the pixel structure of the SLM), and the spatial filter **SF**₁, that selects the first diffracted order of the preparation mask displayed in **SLM**₁. After **SLM**₂, the lens **L**₂ is placed at a distance equal to its focal length f_2 . In this way, the spherical reference wavefront, which is diffracted by the central pixel,

is collimated and it interferes with the tested wavefront at plane Π_i . Finally, the interferograms were detected by a high-sensitivity camera based on complementary metal-oxide semiconductor (**sCMOS**) technology placed at the image plane Π_i . The camera used is a Thorlabs Quantalux sCMOS with HD definition.

IV. RESULTS

We present here the experimental results that validate our method to carry out spatial qudit tomography from a minimum number of measurements. Additionally, in subsection IV B we present a proof-of-principle demonstration that the proposed technique can be used to correct phase aberrations such as the one that undergoes the free propagation of photonic states under turbulence.

A. Reconstruction of spatial qudits

In figure 4 we show, as an example, the interferograms registered for a particular qudit state of dimension $d = 6$ with uniform real amplitudes, i.e., where the coefficients c_k in equation (10) meet that $|c_k|^2 = 1/d$, and its phases were arbitrarily selected. The full characterization of the state is obtained from a four step PSI, $N = 4$. Figure 4a shows the intensity distribution registered on Π_i . The rectangles in yellow indicate the regions of interest (ROIs) from where the phase and intensity of each slit are evaluated. It is worth noting that the dark zones surrounding the slits are the result of diffraction in the borders, but inside the ROIs both, amplitude and phase of the coefficients c_k , are correctly represented. Figure 4b shows the interferogram corresponding to a phase shift $\alpha_2 = \pi$, while the red circle indicates the circular pupil of radius R mathematically described by the circle function in equation (11). The light intensity *outside* the pupil in this interferogram corresponds to the reference beam. As it was explained in II A, in order to estimate the reference amplitude $|K|$ we have to know the magnitude of $C(x, y)$, shown in figure 4c, at those points where the input wavefront is zero. The white arrow marks an area in which C_0 can be estimated. Finally, figure 4d shows the phase map corresponding to the zone delimited by the outer yellow rectangle drawn in figure 4a. The phase value assigned to each slit is obtained by averaging within each ROI.

To assess the feasibility of the method we reconstructed a large number of pure qudits of dimension $d = 6$ randomly chosen. As a figure of merit we used the fidelity, that is defined, for pure states, as $F(\Phi, \Psi) = |\langle \Phi | \Psi \rangle|$, where $|\Phi\rangle$ represents the state to be prepared, and $|\Psi\rangle$ the state that is reconstructed [2]. Ideally, $F = 1$. The states were selected with the Haar measure in a Hilbert space of dimension $d = 6$. The histogram in figure 5 shows the occurrence fidelity for 150 states. The mean fidelity is $\bar{F} = 0.95$, with a standard deviation of $\sigma_F = 0.02$. This fidelity value is comparable to those obtained by means

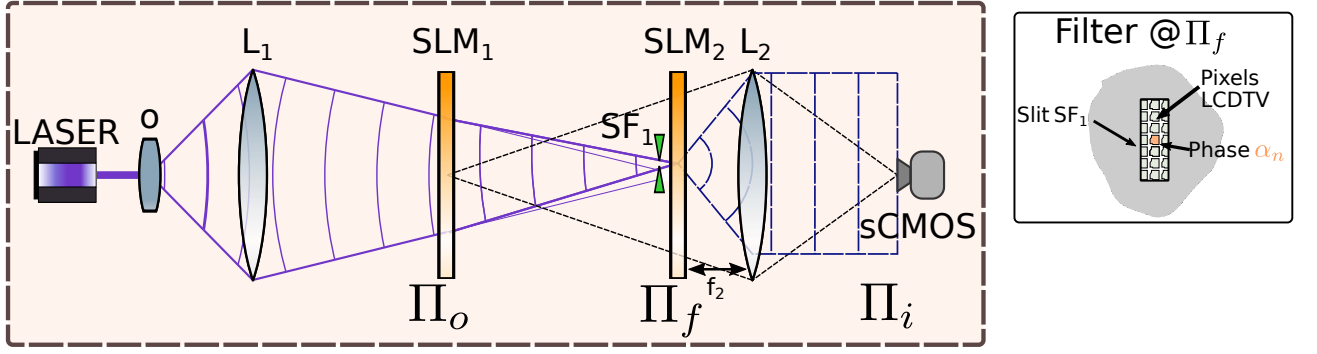


FIG. 3: Experimental setup. The light source is a 405nm cw laser diode, attenuated down to the single photon level. Lenses L s conform a convergent optical processor. $SLMs$ are phase-only spatial light modulators and SF_1 is a spatial filter. The interferograms are detected by a high-sensitivity **sCMOS** camera. The detail shows the filter placed in the Fourier Plane Π_f : the slit SF_1 selects the first diffracted order in the spatial qudit preparation, while the central pixel of SLM_2 introduces the PSI phase retardation α_n .

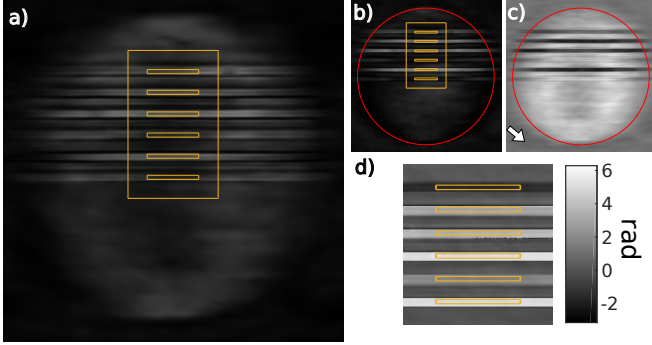


FIG. 4: Example of a measurement for a qudit of dimension $d = 6$ with uniform amplitudes. (a) Interferogram corresponding to a phase shift $\alpha_0 = 0$, which matches the intensity distribution of the aperture $B(\mathbf{x})$. The inner yellow rectangles represent the ROIs where the phase of each slit is evaluated. The outer rectangle demarcates the zone zoomed in (d). (b) Interferogram corresponding to a phase shift $\alpha_2 = \pi$. The red circle represents the pupil of radius R . (c) 2D map of corresponding to the term $C(x, y)$. The white arrow points the area, outside the pupil, in which $|K|$ is evaluated. (d) Reconstructed phase map, the value assigned to each slit is obtained by averaging within each ROI.

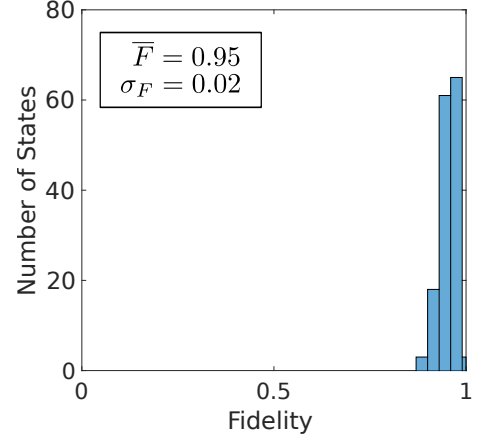


FIG. 5: Histogram of the reconstruction fidelities for 150 random pure states of dimension $d = 6$. The mean fidelity is $\bar{F} = 0.95$, and the standard deviation is $\sigma_F = 0.02$.

B. Turbulence correction

Since the PDI allows us to know the phase distribution of each point of the wavefront, it is possible to evaluate deviations from the ideal situation in the region outside the slits. As this region does not carry information about the states, its phase distribution should be constant and known *a priori* by the receiver. Then, the obtained information about the aberrations present in this region can be used to estimate and correct aberrations present in the ROIs of the wavefront. In particular, we are going to deal with a case of great interest in free-space quantum communications, such as the influence of a turbulent medium on the information encoded and transmitted in the quantum state of photons.

In a free-space communication system the sender encodes the information in some degree of freedom of the wavefront, the signal travels a given distance through free

of other QST methods [17, 19], with the advantage of being implemented from a very stable optical architecture, which also allows to carry out the characterization through only 4 measurements, regardless of the dimension of the system.

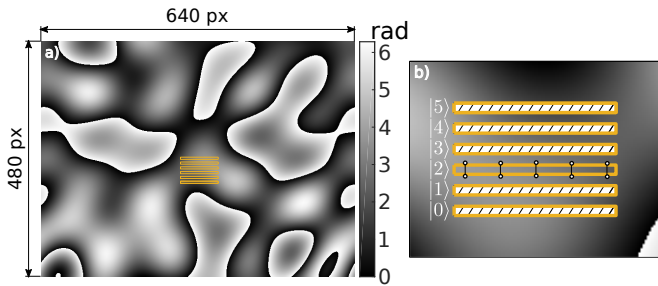


FIG. 6: (a) Example of a turbulence phase mask displayed in the same modulator (SLM_1) used to generate the slit states. This mask corresponds to an ensemble with Fried's parameter $r_0 = 1.9$ mm. The yellow rectangles represent the position of the slits. (b) Schematics for the aberration estimation procedure inside the slit. Given that the phase aberration can only be evaluated on the background region, the phase for every point of the slit is obtained by interpolating the values nearest to the horizontal borders. The concept is illustrated for the slit $|2\rangle$.

space, and is collected by means of a telescope-like system by the receiver. The turbulence, which entails random changes of the local pressure, and hence in the refraction index, distorts the received signal. In the *phase screen approximation* [37], valid when the turbulence is not too strong [38], all the effects of the turbulence can be represented as a random additive phase on the input of the receiver's telescope. The stochastic set of phase masks is described by the Kolmogorov theory, and follow the spatial structure function [39]

$$\begin{aligned} \mathcal{D}_\varphi &= \langle [\varphi(\mathbf{r}) - \varphi(\mathbf{r} + \delta\mathbf{r})]^2 \rangle \\ &= 6.88(\delta r/r_0)^{5/3}, \end{aligned} \quad (12)$$

where $\langle \rangle$ denotes the average over the random ensemble, \mathbf{r} and $\mathbf{r} + \delta\mathbf{r}$ represent the position of two points in the transverse plane of the telescope input, and r_0 is the Fried's parameter, that represents the typical length of spatial correlation of the phase fluctuation.

In order to study the effect of turbulence over the propagation of our slit states, an ensemble of phase masks verifying equation (12) was generated as a linear combination of normal modes with random phases that obey an appropriate power law [24, 40]. The amplitude of the m normal mode was selected to be $A_m = A_0 e^{-1/4m}$, where A_0 is the amplitude of the fundamental mode. The phase of each mode is randomly changed in a time $T_m = T_0 e^{-1/3m}$, where T_0 is the time for the fundamental mode. The power law variations of the mode parameters ensure the appropriate phase structure relation. As an example, one of the random phase mask of this ensemble is shown in figure 6a. The empirical model of Hufnagel-Valley [41] allows us to relate the Fried's parameter with the height above the sea level in which the transmission takes place. In our case, we have chosen

$r_0 = 1.9$ mm, which is compatible with a 500 m long link at 647 m. Thus, to simulate a quantum state reconstruction in presence of turbulence, we programmed, in the SLM_1 , the nominal state to be reconstructed with the addition of a random phase mask compatible with equation (12). Then the four-step PSI is performed assuming that the turbulent-induced phase aberration does not change during the acquisition. The validity of this assumption will depend both on the acquisition rates of the camera and commutation time of the phase in the PDI filter. Although in our case this time is limited by the refresh rate of the LCD (60 Hz), there are alternative electro-optical PDI filters with refresh rates up to MHz [42], and sCMOS cameras can exceed 1000 fps in small ROIs.

Let us describe the method to correct the phase aberrations introduced by the turbulence. As we explained in section II, the background signal added to the codification of our photonic states allows us to reconstruct the phase distribution of the whole region within the circular pupil. Thus, we can accurately estimate the turbulence-induced phase distortion *outside* the ROIs. Inside the ROIs we are unable to discriminate the phase aberrations from the unknown phase of the slit, and then, the turbulence-induced phase distortion cannot be estimated directly. However, the information of the phase *outside* the ROI can be used to interpolate it inside of each slit. Figure 6b exemplify this idea for the slit assigned to the state $|2\rangle$. Along the slit, the phase values corresponding to the points in the circles (outside the ROI) are used to calculate the phase values of the points belonging to the straight line (inside the ROI) by means of a linear interpolation. In that way, the full map of the phase aberrations can be reconstructed and subtracted from the full phase distribution obtained by PSI.

To test the capability of the method to correct the turbulence aberrations we have performed the reconstruction of 100 random states of dimension $d = 6$. Figure 7a shows the histogram for the reconstruction fidelity when the effects of the turbulence are not corrected. A significantly lower mean fidelity ($\overline{F}_{uc} = 0.8$) than in the case without turbulence, and a higher standard deviation ($\sigma_{F_{uc}} = 0.19$), are obtained. Figure 7b shows the occurrence of reconstruction fidelity for the same states after being processed with the described correction method. We can say that there is an excellent enhancement in the quality of the reconstruction supported by a mean fidelity of $\overline{F}_c = 0.95$ and a standard deviation $\sigma_{F_c} = 0.03$, both values comparable to those of the situation without turbulence.

V. CONCLUSIONS

We have presented a method to reconstruct pure spatial qudits codified in the discretized transverse momentum of a photon field (usually called slit states), that is based on a point diffraction interferometer. This archi-

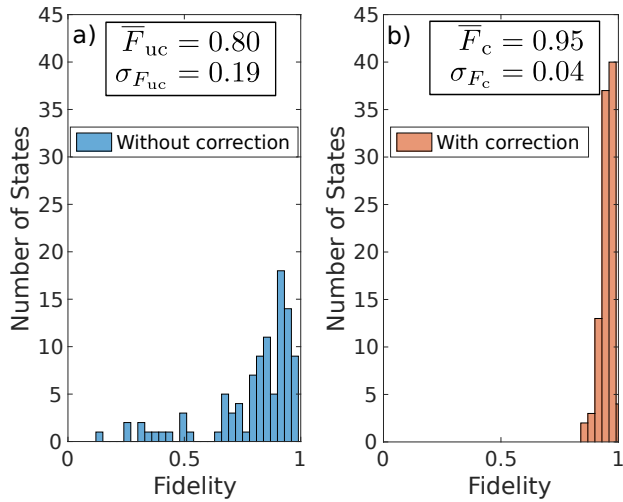


FIG. 7: (a) Histogram of fidelity reconstruction for 100 random states ($d = 6$) affected by a turbulence with $r_0 = 1.9$ mm. Its mean fidelity is low, $\bar{F}_{uc} = 0.8$. (b) Histogram of the reconstruction fidelity for the same 100 states *after* applying the phase correction method. The mean fidelity $\bar{F}_c = 0.95$ is comparable to the case without turbulence.

ture results in an experimental setup easy to align, and very stable against vibrations and air turbulence.

As remarkable property, the measurements can be parallelized by using a multipixel detector, in which case only four interferograms are required to reconstruct any pure state regardless of the dimension of the system. To this end we propose an alternative encoding for the slit states that includes an uniform background that plays the role of reference beam. This allows to accurately reconstruct the phase of the whole photonic wavefront, and estimate possible aberrations.

We have experimentally tested the proposed method in the reconstruction of states of dimension $d=6$, obtaining a mean fidelity value $\bar{F} = 0.95$. Finally, we presented a proof-of-principle demonstration that the method can be used to correct the influence of turbulence in a free-space communication. To that end, we experimentally simulated a turbulent channel using random phase masks. In the case of weak turbulence, and after correction, we recovered mean fidelity values comparable to the case without turbulence.

ACKNOWLEDGMENTS

This work was supported by Universidad de Buenos Aires (UBACyT Grant No. 20020170100564BA). Q.P.S. was supported by a CONICET Fellowship.

-
- [1] G. Tóth and I. Apellaniz, *Journal of Physics A: Mathematical and Theoretical* **47** (2014), 10.1088/1751-8113/47/42/424006, arXiv:1405.4878.
 - [2] M. A. Nielsen and I. L. Chuang, *Quantum Computing and Quantum Information* (Cambridge University Press, England, 2000).
 - [3] J. I. Cirac, P. Zoller, H. J. Kimble, and H. Mabuchi, *Physical Review Letters* **78**, 3221 (1997), arXiv:9611017 [quant-ph].
 - [4] N. Gisin, G. Ribordy, W. Tittel, and H. Zbinden, *Reviews of Modern Physics* **74**, 145 (2002).
 - [5] R. Ursin, T. Jennewein, M. Aspelmeyer, R. Kaltenbaek, M. Lindenthal, P. Walther, and A. Zeilinger, *Nature* **430**, 849 (2004).
 - [6] B. Hensen, H. Bernien, A. E. Dreaú, A. Reiserer, N. Kalb, M. S. Blok, J. Ruitenbergh, R. F. Vermeulen, R. N. Schouten, C. Abellán, W. Amaya, V. Pruneri, M. W. Mitchell, M. Markham, D. J. Twitchen, D. Elkouss, S. Wehner, T. H. Taminiau, and R. Hanson, *Nature* **526**, 682 (2015).
 - [7] D. James, P. Kwiat, W. Munro, and A. White, *Physical Review A* (2001).
 - [8] W. K. Wootters and B. D. Fields, *Annals of Physics* **191**, 363 (1989).
 - [9] R. B. A. Adamson and A. M. Steinberg, *Physical review letters* **105**, 030406 (2010).
 - [10] N. J. Cerf, M. Bourennane, A. Karlsson, and N. Gisin, *Physical Review Letters* **88**, 127902 (2002), arXiv:0107130 [arXiv:quant-ph].
 - [11] A. C. Dada, J. Leach, G. S. Buller, M. J. Padgett, and E. Andersson, *Nature Physics* **7**, 677 (2011).
 - [12] J. Mower, Z. Zhang, P. Desjardins, C. Lee, J. H. Shapiro, and D. Englund, *Physical Review A* **87**, 1 (2013), arXiv:1210.4501.
 - [13] T. Zhong, H. Zhou, R. D. Horansky, C. Lee, V. B. Verma, A. E. Lita, A. Restelli, J. C. Bienfang, R. P. Mirin, T. Gerrits, S. W. Nam, F. Marsili, M. D. Shaw, Z. Zhang, L. Wang, D. Englund, G. W. Wornell, J. H. Shapiro, and F. N. Wong, *New Journal of Physics* **17** (2015), 10.1088/1367-2630/17/2/022002.
 - [14] M. Mirhosseini, O. S. Magaña-Loaiza, M. N. O'Sullivan, B. Rodenburg, M. Malik, M. P. J. Lavery, M. J. Padgett, D. J. Gauthier, and R. W. Boyd, *New Journal of Physics* **17**, 033033 (2015), arXiv:1402.7113.
 - [15] D. Martínez, M. A. Solís-Prosser, G. Cañas, O. Jiménez, A. Delgado, and G. Lima, *Physical Review A* **99**, 1 (2019).
 - [16] G. Cañas, M. Arias, S. Etcheverry, E. S. Gómez, A. Cabello, G. B. Xavier, and G. Lima, *Physical review letters* **113**, 090404 (2014).
 - [17] D. Goyeneche, G. Cañas, S. Etcheverry, E. S. Gómez, G. B. Xavier, G. Lima, and A. Delgado, *Physical Review Letters* **115**, 090401 (2015), arXiv:1411.2789.
 - [18] C. Carmeli, T. Heinosaari, M. Kech, J. Schultz, and A. Toigo, *Epl* **115** (2016), 10.1209/0295-5075/115/30001, arXiv:1604.02970.
 - [19] Q. P. Stefano, L. Rebón, S. Ledesma, and C. Iemmi, *Optics Letters* **44**, 2558 (2019).

- [20] N. Gisin and R. Thew, *Nature Photonics* **1**, 165 (2007), arXiv:0703255 [quant-ph].
- [21] L. Neves, G. Lima, J. G. Aguirre Gómez, C. H. Monken, C. Saavedra, and S. Pádúa, *Physical Review Letters* **94**, 100501 (2005).
- [22] S. Etcheverry, G. Cañas, E. S. Gómez, W. A. T. Nogueira, C. Saavedra, G. B. Xavier, and G. Lima, *Scientific reports* **3**, 2316 (2013).
- [23] Q. Pears Stefano, L. Rebón, S. Ledesma, and C. Iemmi, *Physical Review A* **96**, 1 (2017), arXiv:1707.03306.
- [24] J. J. M. Varga, L. Rebón, Q. Pears Stefano, and C. Iemmi, *Optics Letters* **43**, 4398 (2018), arXiv:1806.06128.
- [25] W. Linnik, in *Dokl. Akad. Nauk, SSSR*, Vol. 1 (1933) pp. 21–33.
- [26] C. Koliopoulos, C. R. Hayslett, O. Kwon, R. Shagam, and J. C. Wyant, *Optics Letters* **3**, 118 (1978).
- [27] P. Naulleau, K. A. Goldberg, S. H. Lee, C. Chang, D. Attwood, and J. Bokor, in *AIP Conference Proceedings*, Vol. 521, edited by P. Pianetta, J. Arthur, and S. Brennan (AIP, Standford, 2000) pp. 66–72.
- [28] C. R. Mercer and K. Creath, *Applied Optics* **35**, 1633 (1996).
- [29] C. Iemmi, A. Moreno, J. Nicols, and J. Campos, *Optics Letters* **28**, 1117 (2003).
- [30] C. Ramírez, E. Otón, C. Iemmi, I. Moreno, N. Bennis, J. M. Otón, and J. Campos, *Optics Express* **21**, 8116 (2013).
- [31] K. Creath, *Progress in Optics* **26**, 349 (1988).
- [32] L. Neves, S. Pádúa, and C. Saavedra, *Physical Review A* **69** (2004), 10.1103/PhysRevA.69.042305.
- [33] M. A. Solís-Prosser, A. Arias, J. J. M. Varga, L. Rebón, S. Ledesma, C. Iemmi, and L. Neves, *Optics Letters* **38**, 4762 (2013).
- [34] J. J. Varga, S. Ledesma, C. Iemmi, and L. Rebón, *Physical Review A* **96**, 34 (2017), arXiv:arXiv:1706.00920v1.
- [35] A. Marquez, C. Iemmi, I. S. Moreno, J. A. Davis, J. Campos, and M. J. Yzuel, *Optical Engineering* **40**, 2558 (2001).
- [36] J. J. M. Varga, L. Rebón, M. A. Solís-Prosser, L. Neves, S. Ledesma, and C. Iemmi, *Journal of Physics B: Atomic, Molecular and Optical Physics* **47**, 225504 (2014).
- [37] R. W. Boyd, B. Rodenburg, M. Mirhosseini, and S. M. Barnett, *Optics Express* **19**, 18310 (2011).
- [38] B. Rodenburg, M. Lavery, M. Malik, M. O’Sullivan, M. Mirhosseini, M. Padgett, and R. W. Boyd, *Optics InfoBase Conference Papers* **19**, 18310 (2011).
- [39] D. L. Fried, *Journal of the Optical Society of America* **56**, 410 (1966).
- [40] J. J. M. Varga, *Uso de moduladores espaciales de luz para la implementación y caracterización de estados y procesos cuánticos*, Ph.D. thesis, Universidad de Buenos Aires (2018).
- [41] G. C. Valley, *Applied Optics* **19**, 574 (1980).
- [42] M. Paturzo, S. Grilli, and P. Ferraro, *Optical Measurement Systems for Industrial Inspection V* **6616**, 66160F (2007).